Backstepping Sliding Mode Tracking Controller Design and Experimental Application to an Electromechanical System

Ramazan Coban

Cukurova University, Department of Computer Engineering, 01330 Balcali, Saricam, Adana, Turkey (Tel: +903223387101x15; e-mail: rcoban@cu.edu.tr).

Abstract: In this paper, a backstepping sliding mode control (BSMC) system based on the Lyapunov stability criterion is put forward to control the angular velocity of an electromechanical system to closely track the desired trajectory in spite of parameter uncertainties, nonlinear dynamics, and disturbances. In addition, for comparison purposes a conventional sliding mode controller and a backstepping controller are designed. Experimental results of the proposed BSMC are compared with those of the other two controllers. The proposed BSMC accomplishes satisfactory trajectory tracking performance, and it is more robust pertaining to parametric uncertainties and disturbances than the others.

Keywords: Sliding mode; Backstepping; Backstepping sliding mode; Nonlinear control; Electromechanical system.

1. INTRODUCTION

In recent years, there has been a growing interest and research in design of robust controllers for the nonlinear dynamic systems with matched and unmatched parameter uncertainties and disturbances (Davila, 2013). The design of robust controllers for such nonlinear systems is one of the most challenging tasks for control engineers, practitioners, and scientists. They have recommended some design solutions by using different approaches such as sliding mode control (SMC), adaptive control (AC), and backstepping control (BSC). One of the most flourishing control approaches to overcome the negative effects of uncertainties on the nonlinear systems is sliding mode control. Sensitivity of the nonlinear plant under sliding mode control with respect to uncertainties and disturbances is reduced in return for chattering in many practical situations (Rubagotti et al., 2011). Sliding mode control can tackle uncertainties and disturbances by the knowledge about their lower and upper bounds to need no parameter adaptation. The other approach to dealing with uncertainty is adaptive control. The fundamental goal of adaptive control is to retain reliable performance of a dynamic system in the presence of parameter uncertainties by using on-line parameter adaptation without prior knowledge about the unknown parameters. Due to its on-line adaptation ability, adaptive control for a plant with uncertainties in constant or slowly-varying parameters is superior to sliding mode control. Nonetheless, sliding mode control outperforms adaptive control under disturbances, uncertainties in quickly varying parameters, and unstructured uncertainties (Slotine et al., 1991).

Stability of the overall system and convergence of the parameters to be adapted to ideal ones using parameter update law may be easily achieved by Lyapunov-based adaptive control design. However, it can be only applied to linear systems with relative degree one or two and to nonlinear systems with the number of integrators between the control input and the parameter to be adapted less than two. This drawback can be eliminated by the recursive design referred to as backstepping control (Krstic et al., 1995). The rationale behind backstepping is to design the control input to stabilize the overall system by cancellation of all destabilizing terms in each first-order subsystem obtained from the nth order system in a lower triangular form constructing a backstepping change of variables in a recursive fashion. Backstepping control design takes advantage of a step by step procedure and Lyapunov direct method since it views some of the system states as virtual controls until the actual control is reached (Krstic et al., 1995; Krstic et al., 2008). However, it is not robust against uncertainties. So as to exploit the advantages of robustness presented by the sliding mode control and Lyapunov based recursive design by the backstepping control, these two methods can be associated. The association of the backstepping design and the sliding mode control referred to as backstepping sliding mode control (BSMC) is an effective method alternative to the adaptive control for nonlinear systems with both matched and unmatched uncertainties and disturbances (Davila, 2013; Madani et al., 2006; Adhikary et al., 2013; Lu et al., 2011; Zinober et al., 1996).

Generally, electromechanical systems appear in industrial applications requiring adjustable speed regulation and frequent starting, braking and reversing, such as robotics, numeric control machines, and industrial tools (Sahab et al., 2012; Damiano et al., 2004; Payam, 2006). The main part of an electromechanical system is the dc motor as an actuator. It is important to control its position or velocity under load variations and disturbances. The well-known linear control necessitates fairly accurate information about electromechanical system parameters to accomplish the desired compromise between performance and disturbance rejection. Because of unknown parameters or uncertainties in

parameters due to different load conditions, performance of an electromechanical system degrades (Damiano et al., 2004; Chaouch et al., 2006). In this paper, in order to overcome this deficiency, robust control methods are used. A nonlinear backstepping sliding mode controller based on the Lyapunov stability theorem is designed in order for output of an electromechanical system to track the desired trajectory in spite of parametric uncertainties, nonlinear dynamics, and disturbances. The proposed BSMC is designed so that the stability of the whole closed-loop system during the reaching phase and sliding phase is ensured. The proposed control method has been experimentally applied to control an electromechanical system. Experimental results of the proposed design demonstrate that the trajectory tracking performance is increased in existence of uncertainties and disturbances and at the same time the stability is maintained. Furthermore, for comparison purposes a conventional sliding mode controller and a backstepping controller are designed since there does not exist a comprehensive comparison study among these three designs in literature. Experimental results of the proposed backstepping sliding mode controller are compared with those of the both controllers. The paper is organized as follows. The experimental set-up and mathematical model of the electromechanical system are given in Section 2. Design methods which are backstepping, conventional sliding mode, and backstepping sliding mode controllers are introduced in section 3. In section 4, experimental applications and results of the proposed backstepping sliding mode controller as well as conventional sliding mode and backstepping controllers, and also comparison results are provided. Finally, the conclusions are given in section 5.

2. MATHEMATICAL MODEL OF THE ELECTROMECHANICAL SYSTEM AND THE EXPERIMENTAL SET-UP

In this paper, the Precision Modular Servo (PMS) setup developed by Feedback Instruments is considered as a test bed. The PMS consists of a brushed dc motor, digital encoder, power supply, pre-amplifier, servo-amplifier, attenuator, output potentiometer, gearbox/tachometer, and analogue control interface units as shown in Fig. 1. The set-up allows designers to test their controllers in real time (Kesarkar et al., 2013). The electromechanical system PMS consists of essentially electrical and mechanical units as seen in the figure. The input-output signals in the system are transmitted to the computer via a data acquisition card. The output speed is measured by a tachometer that provides an output voltage proportional to the speed. Digital encoder measures precisely the motor angular position. The digital data from the encoder are conducted to the I/O board. Pre-amplifier supplies the correct signal range to the servo amplifier which provides the controlled power to the DC motor. Interface unit is employed to scale the analogue input and output to the I/O board in the computer to the true operating range. Attenuator is used to set the input to the motor control circuit to the true operating level. Output potentiometer is used as a visual display of motor (gearbox shaft) position. The electromechanical system under consideration operates at control (input) voltage in the range -2.5 V and +2.5 V with a maximum no-load speed of 4050 rpm (Feedback Instruments).

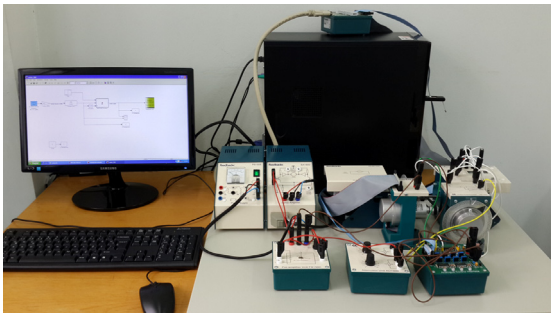

Fig. 1. A photograph of the Precision Modular Servo (PMS) setup.

The mechanical and electrical components consisting of tachometer/gearbox, digital encoder, output potentiometer, a brake disc, transmission belt, and some couplings which are directly connected to the shaft place some additional load effects on the ideal dc brushed motor. These mechanical and electrical parts influence basically moment of inertia and viscous friction of the dc motor. As a result of the load effects on the real experimental system, moment of inertia J_l and viscous friction d_l are included in the motor model equations. A complete mathematical model of the electromechanical system can be derived using mechanical and electrical equations. By Kirchhoff's voltage and Newton's rotational motion laws, one can get the following total torque and voltage equations

$$(J_m + J_l)\ddot{\theta}(t) = \sum \tau_i(t) = -(d_m + d_l)\dot{\theta}(t) + K_t i(t) \tag{1}$$

$$v(t) = L\frac{di(t)}{dt} + Ri(t) + K_b\dot{\theta}(t) \tag{2}$$

where J_m and J_l are the moment of inertia constants; d_m and d_l are the viscous friction constants; K_t is the torque constant; $\dot{\theta}(t)$ is angular shaft velocity; K_b is an electromotive force constant; v is the armature voltage; R is resistance; L is inductance; t is the time. One can rewrite (1) and (2) in the following form:

$$\begin{aligned} \frac{d\dot{\theta}(t)}{dt} &= -\frac{(d_m + d_l)}{(J_m + J_l)}\dot{\theta}(t) + \frac{K_t}{(J_m + J_l)}i(t), \\ \frac{di(t)}{dt} &= -\frac{R}{L}i(t) - \frac{K_b}{L}\dot{\theta}(t) + \frac{1}{L}v(t) \end{aligned} \tag{3}$$

Let us use $\omega(t)$ instead of $\dot{\theta}(t)$ in (3) and then take its Laplace transform:

$$\begin{aligned} S\omega(S) &= -\frac{(d_m + d_l)}{(J_m + J_l)}\omega(S) + \frac{K_t}{(J_m + J_l)}i(S), \\ i(S) &= -\frac{K_b}{SL + R}\omega(S) + \frac{1}{SL + R}v(S) \end{aligned} \tag{4}$$

Substituting the second equation into the first one in (4), the following equation is obtained:

$$S^2\omega(S) = -[\frac{R}{L} + \frac{(d_m + d_l)}{(J_m + J_l)}]S\omega(S) - \frac{(d_m + d_l)R + K_t K_b}{L(J_m + J_l)}\omega(S) + \frac{K_t}{L(J_m + J_l)}v(S) \quad (5)$$

Taking the inverse Laplace transform of (5) and then including the additional gain K_{amp} introduced by the amplifiers, and converting the motor angular velocity from rad/s to rpm, the following equation is obtained:

$$\ddot{\omega}(t) = -[\frac{R}{L} + \frac{(d_m + d_l)}{(J_m + J_l)}]\dot{\omega}(t) - \frac{(d_m + d_l)R + K_t K_b}{L(J_m + J_l)}\omega(t) + \frac{K_{amp} K_t T_{rpm}}{L(J_m + J_l)}v(t) \quad (6)$$

where $T_{rpm} = 60/(2\pi)$ and $K_{amp} = 9.6$. The servo motor model parameters are taken from the datasheet of Feedback Instruments and presented in Table 1 (Feedback Instruments) but moment of inertia J_l and viscous friction d_l due to the load effects of some electrical and mechanical parts on the real electromechanical system are determined by trial and error using a measured input-output data set and simulating the system model. They are given in Table 2. With help of these parameters response of the basic motor model gets closer to that of the real electromechanical system. Despite there still exists a difference between responses of the real system and model, it is rejected by a robust controller to be designed in the succeeding subsections.

Table 1. Values of the electromechanical system parameters.

Parameter	Value
Moment of inertia of the motor J_m	0.0000140 kgm^2
Torque constant K_t	0.052 Nm/A
Electromotive force constant K_b	0.057 Vs/rad
Viscous friction of the motor d_m	0.000001 Nms/rad
Resistance R	2.5 Ω
Inductance L	0.0025 mH

Table 2. Values of the parameters for load effects and dead-zone nonlinearity.

Parameter	Value
Moment of inertia of load J_l	0.0001 kgm^2
Viscous friction of load d_l	0.0005 Nms/rad
Constant slope for dead-zone m_d	1
Constant for dead-zone off_p	0.1 V
Constant for dead-zone off_n	0.15 V

Although the mathematical model of the electromechanical system in (6) is linear, the real one is nonlinear due to dead-zone (static friction), backlash, and other nonlinear elements. Static friction is influenced by the mechanical setup of the electromechanical system. Dead-zone nonlinearity with negligible fast dynamics can be modeled by (Tao et al., 1994)

$$v(t) = \wp(u(t)) = \begin{cases} m_d(u(t) - off_p) & \text{if} \quad u(t) \geq off_p \\ 0 & \text{if} \quad off_n \leq u(t) \leq off_p \\ m_d(u(t) - off_n) & \text{if} \quad u(t) \leq off_n \end{cases} \quad (7)$$

where m_d is the constant slope, off_n and off_p are constant parameters depending on the mechanical properties of the electromechanical system. Values of these constants are given in Table 2, as well. It is assumed here that the dead-zone parameters are within known limits. One can rewrite the dead-zone model in (7) as (Guo et al., 2012)

$$v(t) = \wp(u(t)) = m_d u(t) + \tilde{n}_d(u(t)) \quad (8)$$

where $\tilde{n}_d(u(t))$ is dead-zone modelling error and it satisfies $|\tilde{n}_d| \leq \hbar$ where $\hbar = \max\{(m_d off_p)_{\max}, -[(m_d off_n)_{\min}]\}$ (Zhonghua et al., 2006). Including this dead-zone nonlinearity model into (6) one can get

$$\ddot{\omega}(t) = -[\frac{R}{L} + \frac{(d_m + d_l)}{(J_m + J_l)}]\dot{\omega}(t) - \frac{(d_m + d_l)R + K_t K_b}{L(J_m + J_l)}\omega(t) + \frac{K_{amp} K_t T_{rpm}}{L(J_m + J_l)}[m_d u(t) + \tilde{n}_d(t)] \quad (9)$$

Composing of the model with dead-zone nonlinearity, unmatched uncertainties, and disturbances, the electromechanical system can be modeled as a class of nonlinear dynamical system by

$$\ddot{\omega}(t) = -[\frac{R}{L} + \frac{(d_m + d_l)}{(J_m + J_l)}]\dot{\omega}(t) - \frac{(d_m + d_l)R + K_t K_b}{L(J_m + J_l)}\omega(t) + \frac{K_{amp} K_t T_{rpm}}{L(J_m + J_l)}[m_d u(t) + \tilde{n}_d(t)] + \tilde{d}(x,t) \quad (10)$$

where $\tilde{d}(x,t)$ is the sum of unmatched uncertainties and external disturbances. Taking $\mathbf{x} = [x_1, x_2]^T = [\omega, \dot{\omega}]^T$ as state vector, the following general nonlinear dynamical equation is obtained:

$$\dot{x}_1(t) = x_2(t)$$
$$\dot{x}_2(t) = f(\boldsymbol{x},t) + g(\boldsymbol{x},t)u(t) + d(\boldsymbol{x},t) \quad (11)$$

where $f(\boldsymbol{x},t) = f_0(\boldsymbol{x},t) + \nabla f_0(\boldsymbol{x},t)$, $\nabla f_0(x,t)$ is matched (parametric) uncertainties with constant parameter ∇, $f_0(\boldsymbol{x},t) = -[\frac{R}{L} + \frac{(d_m + d_l)}{(J_m + J_l)}]x_2(t) - \frac{(d_m + d_l)R + K_t K_b}{L(J_m + J_l)}x_1(t)$, $g(\boldsymbol{x},t) = \frac{K_{amp} K_t T_{rpm} m_d}{L(J_m + J_l)}$ is constant and has positive sign, $d(\boldsymbol{x},t) = \frac{K_{amp} K_t T_{rpm}}{L(J_m + J_l)}\tilde{n}_d(t) + \tilde{d}(\boldsymbol{x},t)$, and $|d(\boldsymbol{x},t)| \leq \Upsilon$, Υ is a positive constant.

3. DESIGN METHODS

In the following subsections, backstepping control, conventional sliding mode control, and backstepping sliding mode control proposed for the electromechanical system are briefly presented.

3.1 Backstepping Control Design

For the backstepping control design, neglecting the sum of unmatched uncertainties, external disturbances, and dead-zone nonlinearity ($d(\boldsymbol{x},t)$) let us rewrite the system in (11) as follows:

$$\begin{aligned}\dot{x}_1(t) &= x_2(t)\\ \dot{x}_2(t) &= f(\boldsymbol{x},t)+g(\boldsymbol{x},t)u(t)\\ y(t) &= x_1(t)\end{aligned} \tag{12}$$

where $\mathbf{x}=[x_1,x_2]^T$ is the state; y is output; and u is the control input. The functions f and g are smooth in a domain of interest and known. It is intended to design a tracking control law for the electromechanical system. Let us define tracking error $e_1(t)=x_1(t)-r(t)$ where $r(t)$ is reference trajectory. Derivative of the tracking error with respect to time is $\dot{e}_1(t)=\dot{x}_1(t)-\dot{r}(t)=x_2(t)-\dot{r}(t)$. Starting with the first component in (11) one can view $x_2(t)$ as virtual input to design the feedback control $x_2(t)=\alpha_1(e_1,\dot{r})$ to asymptotically track the reference trajectory. Therefore with $x_2(t)=\alpha_1(e_1,\dot{r})=-k_1e_1(t)+\dot{r}(t)$ one can get

$$\dot{e}_1(t)=-k_1e_1(t) \tag{13}$$

Selecting a smooth and positive definite Lyapunov function candidate $V_1(e_1)=\frac{1}{2}e_1^2(t)$, one obtains

$$\begin{aligned}\dot{V}_1(e_1) &= e_1(t)\dot{e}_1(t)=e_1(t)(-k_1e_1(t))\\ &= -k_1e_1^2(t)\le 0,\ \forall(e_1\neq 0)\in\mathcal{R}\end{aligned} \tag{14}$$

where $k_1>0$

Hence, the origin of $\dot{e}_1(t)=-k_1e_1(t)$ is globally asymptotical stable. Moreover, it is globally exponentially stable. In order to backstep let us use the change of variables $e_2(t)=x_2(t)-\alpha_1(e_1,\dot{r})=x_2(t)+k_1e_1(t)-\dot{r}(t)$ to transform the system into the following form (Khalil, 2015)

$$\begin{aligned}\dot{e}_1(t) &= -k_1e_1(t)+e_2(t)\\ \dot{e}_2(t) &= -k_1^2e_1(t)+k_1e_2(t)+f(\boldsymbol{x},t)+g(\boldsymbol{x},t)u(t)-\ddot{r}(t)\end{aligned} \tag{15}$$

Consider a composite Lyapunov function candidate $V_2(\boldsymbol{e})=V_1(e_1)+\frac{1}{2}e_2^2(t)$. The derivative of V_2 along the trajectories of the system in (15) is

$$\begin{aligned}\dot{V}_2(\boldsymbol{e}) &= e_1(t)\dot{e}_1(t)+e_2(t)\dot{e}_2(t)\\ &= e_1(t)[-k_1e_1(t)+e_2(t)]+e_2(t)[-k_1^2e_1(t)\\ &\quad +k_1e_2(t)+f(\boldsymbol{x},t)+g(\boldsymbol{x},t)u(t)-\ddot{r}(t)]\\ &= -k_1e_1^2(t)+e_2(t)[e_1(t)-k_1^2e_1(t)\\ &\quad +k_1e_2(t)+f(\boldsymbol{x},t)+g(\boldsymbol{x},t)u(t)-\ddot{r}(t)]\end{aligned} \tag{15}$$

To make $\dot{V}_2(\boldsymbol{e})$ negative definite, the bracketed term multiplying $e_2(t)$ is set to $-k_2e_2(t)$ for $k_2>0$. Hence, the time derivative of Lyapunov function becomes negative definite $\dot{V}_2(\boldsymbol{e})=-k_1e_1^2(t)-k_2e_2^2(t)\le 0,\ \forall(e\neq 0)\in\mathcal{R}$. For stability of the whole system, the state feedback control law is selected as follow:

$$\begin{aligned}u(t) &= \frac{1}{g(\boldsymbol{x},t)}[-k_2e_2(t)-e_1(t)+k_1^2e_1(t)-k_1e_2(t)\\ &\quad -f(\boldsymbol{x},t)+\ddot{r}(t)]\\ &= \frac{1}{g(\boldsymbol{x},t)}[-(1+k_1k_2)e_1(t)-(k_1+k_2)\dot{e}_1(t)-f(\boldsymbol{x},t)\\ &\quad +\ddot{r}(t)]\\ &= \frac{1}{g(\boldsymbol{x},t)}\{-(1+k_1k_2)[x_1(t)-r(t)]-(k_1+k_2)[x_2(t)\\ &\quad -\dot{r}(t)]-f(\boldsymbol{x},t)+\ddot{r}(t)\}\end{aligned} \tag{16}$$

Thus, the origin of the whole system in (15) is globally asymptotical stable. Furthermore, the control law given in (17) makes output $y(t)$ of the system in (12) globally asymptotically track the reference trajectory.

3.2 Sliding Mode Control Design

Sliding mode control based on discontinuous control laws (relays) is an efficient tool to control nonlinear dynamical systems with uncertainties (Utkin et al., 2009). In design, first, switching surface (sliding manifold) equations are chosen according to some performance specifications. Afterwards, a discontinuous feedback control law $u_{sw}(t)$ is determined so that the system trajectory would reach this surface and remain in its vicinity (Bisztyga et al., 2012). Because of motion on the switching surface $s(t)=0$ for $t>0$ one can consider additional control law instead of the discontinuous one. During sliding mode, setting the derivative of $s(t)$ with respect to time to zero ($\dot{s}(t)=0$) the so-called equivalent control $u_{eq}(t)$ is calculated (Utkin et al., 2009). Consequently, the control law in the sliding mode controller design contains both the equivalent control $u_{eq}(t)$ and the switching (discontinuous) control $u_{sw}(t)$ and then one has

$$u(t)=u_{sw}(t)+u_{eq}(t). \tag{17}$$

In order to design a sliding mode tracking control for the electromechanical system in (11) let us first select a sliding surface using the tracking error $e(t)=y(t)-r(t)=x_1(t)-r(t)$

with the output $y(t)=\omega(t)=x_1(t)$ as follows:

$$s(t)=c_1e(t)+\dot{e}(t) \tag{18}$$

For the switching control $u_{sw}(t)$ design satisfying reaching conditions let us select $V(s)=\frac{1}{2}s^2(t)\geq 0$ as a Lyapunov function candidate. The derivative of V along the trajectories of the system in (11) and (19) is

$$\begin{aligned}\dot{V}(s(t))&=\frac{\partial V(s(t))}{\partial s(t)}\frac{\partial s(t)}{\partial t}=s(t)\dot{s}(t)\\&=s(t)[c_1\dot{e}(t)+\ddot{e}(t)]\\&=s(t)[c_1\dot{e}(t)+f(\boldsymbol{x},t)+g(\boldsymbol{x},t)u_{sw}(t)+d(\boldsymbol{x},t)\\&\quad-\ddot{r}(t)]\leq-\beth s(t)\text{sign}(s(t))=-\beth|s(t)|\leq 0\end{aligned} \tag{19}$$

with the switching control law

$$u_{sw}(t)=-\beth\text{sign}(s(t)) \tag{20}$$

where $\beth\geq\left|\frac{c_1[x_2(t)-\dot{r}(t)]+f(\boldsymbol{x},t)+d(\boldsymbol{x},t)-\ddot{r}(t)}{g(\boldsymbol{x},t)}\right|$, and

$$\text{sign}(s)=\begin{cases}1, & s(t)>0\\0, & s(t)=0\\-1, & s(t)<0\end{cases}.$$

Therefore, the system trajectory reaches the sliding surface in finite time and remains therein due to the fact that $\dot{V}(s(t))=-\beth|s(t)|\leq 0$.

For the equivalent control $u_{eq}(t)$ design, if external disturbances and uncertainties are ignored and the derivative of $s(t)$ with respect to time is set to zero, one obtains

$$u_{eq}(t)=\frac{1}{g(\boldsymbol{x},t)}[-c_1\dot{e}(t)-f(\boldsymbol{x},t)+\ddot{r}(t)] \tag{21}$$

Let us consider both the equivalent control $u_{eq}(t)$ and the switching control $u_{sw}(t)$ to prove stability of the controlled system. To this end, let us employ the control law in (18) together with the equivalent control $u_{eq}(t)$ in (22), and choose $V(s)=\frac{1}{2}s^2(t)\geq 0$ as a Lyapunov function candidate. Its time derivative is

$$\begin{aligned}\dot{V}(s(t))&=s(t)[c_1\dot{e}(t)+f(\boldsymbol{x},t)+g(\boldsymbol{x},t)(u_{eq}(t)+u_{sw}(t))\\&\quad+d(\boldsymbol{x},t)-\ddot{r}(t)]\\&=s(t)\{c_1\dot{e}(t)+f(\boldsymbol{x},t)+g(\boldsymbol{x},t)\frac{1}{g(\boldsymbol{x},t)}[-c_1\dot{e}(t)\\&\quad-f(\boldsymbol{x},t)+\ddot{r}(t)]+g(\boldsymbol{x},t)u_{sw}(t)+d(\boldsymbol{x},t)-\ddot{r}(t)\}\\&=s(t)[g(\boldsymbol{x},t)u_{sw}(t)+d(\boldsymbol{x},t)]\\&\leq-K_s s(t)\text{sign}(s(t))=-K_s|s(t)|\leq 0\end{aligned} \tag{22}$$

with the switching control law

$$u_{sw}(t)=-\frac{1}{g(\boldsymbol{x},t)}K_s\text{sign}(s(t)) \tag{23}$$

where $K_s>\Upsilon\geq|d(\boldsymbol{x},t)|$. The stability proof of the system is ended up with the negative definiteness of Lyapunov function V everywhere except on the manifold $s(t)=0$. Then, the controlled system is asymptotically stable according to LaSalle's invariance principle.

Sliding mode control suffers the so-called chattering due to imperfections in switching devices. One of the various methods to reduce chattering is to use a saturation function instead of the signum function. In this case, the switching control is given by

$$u_{sw}(t)=-\frac{1}{g(x,t)}\text{K}_s sat(s/\varepsilon_s) \tag{24}$$

where $sat(\mathfrak{h})=\begin{cases}\mathfrak{h}, & |\mathfrak{h}|\leq 1\\sign(\mathfrak{h}), & |\mathfrak{h}|>1\end{cases}$

3.3 Backstepping Sliding Mode Tracking Control Design

In this subsection, the above mentioned backstepping control and sliding mode control are associated to design a backstepping sliding mode control which realizes the robust control for the electromechanical system with uncertainties and disturbances. Main goal of the controller is to make the output (angular velocity) of the system asymptotically track a given trajectory despite of uncertainties and disturbances. Fig. 2 portraits the proposed backstepping sliding mode control system.

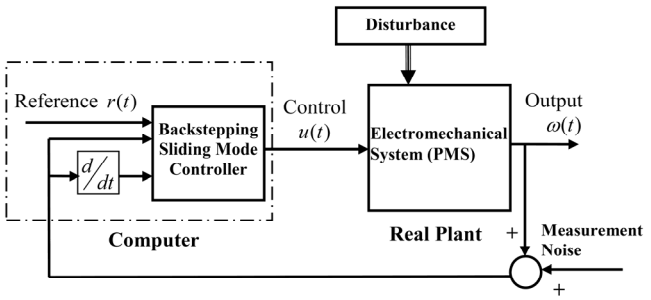

Fig. 2. Block diagram of the proposed backstepping sliding mode control system.

Considering again the electromechanical system given in (11) with the output $y(t)=\omega(t)=x_1(t)$, one can write the tracking error and its time derivative , respectively, in the first step (Liu et al., 2012; Espinoza et al., 2014; Rajendran et al., 2015)

$$\begin{aligned}e(t)&=x_1(t)-r(t)\\\dot{e}(t)&=\dot{x}_1(t)-\dot{r}(t)\end{aligned} \tag{25}$$

Let us select $V_1(e)=\frac{1}{2}e^2(t)>0,\ \forall e\neq 0$ as a Lyapunov function candidate. The derivative of V with respect to time is

$$\dot{V}(e(t))=\frac{\partial V(e(t))}{\partial e(t)}\frac{\partial e(t)}{\partial t}=e(t)\dot{e}(t)=e(t)[x_2(t)-r(t)] \tag{26}$$

One can view $x_2(t)$ as virtual input to design the feedback control $x_2(t)=\alpha(e,\dot{r})$ to asymptotically track the reference trajectory. With choosing $x_2(t)=\alpha(e,\dot{r})=-\varrho_1 e(t)+\dot{r}(t)$ the origin of $\dot{e}(t)=-\varrho_1 e(t)$ is globally exponentially stable since $\dot{V}_1(e)=-\varrho_1 e^2(t)<0,\ \forall(e\neq 0)\in\mathcal{R}$ where $\varrho_1>0$. In order to backstep let us use the change of variables $s(t)=x_2(t)-\alpha(e,\dot{r})=x_2(t)+\varrho_1 e(t)-\dot{r}(t)$ to transform the system into the following form

$$\begin{aligned}\dot{e}(t)&=-\varrho_1 e(t)+s(t)\\ \dot{s}(t)&=-\varrho_1^2 e(t)+\varrho_1 s(t)+f(\boldsymbol{x},t)+g(\boldsymbol{x},t)u(t)+d(\boldsymbol{x},t)\\ &\quad-\ddot{r}(t)\end{aligned} \tag{27}$$

Suppose a composite Lyapunov function candidate $V_2(e,s)=V_1(e)+\frac{1}{2}s^2$. The derivative of V_2 along the trajectories of the system in (28) is

$$\begin{aligned}\dot{V}_2(e,s)&=e(t)[-\varrho_1 e(t)+s(t)]+s(t)[-\varrho_1^2 e(t)+\varrho_1 s(t)\\ &\quad+f(\boldsymbol{x},t)+d(\boldsymbol{x},t)+g(\boldsymbol{x},t)u(t)-\ddot{r}(t)]\\ &=-\varrho_1 e^2(t)-\varrho_2 s^2(t)+s(t)d(\boldsymbol{x},t)-K_{bs}|s|]<0,\\ &\forall(e\neq 0,s\neq 0)\in\mathcal{R}\end{aligned} \tag{28}$$

where $\varrho_2>0$ and with the state feedback control law

$$\begin{aligned}u(t)&=\frac{1}{g(\boldsymbol{x},t)}[-(1+\varrho_1\varrho_2)e(t)-(\varrho_1+\varrho_2)\dot{e}(t)\\ &\quad-f(\boldsymbol{x},t)+\ddot{r}(t)-K_{bs}\text{sign}(s)]\\ &=\frac{1}{g(\boldsymbol{x},t)}[-(1+\varrho_1\varrho_2)(x_1(t)-r(t))-(\varrho_1+\varrho_2)(x_2(t)\\ &\quad-\dot{r}(t))-f(\boldsymbol{x},t)+\ddot{r}(t)-K_{bs}\text{sign}(s)]\end{aligned} \tag{29}$$

where $K_{bs}>\Upsilon\geq|d(\boldsymbol{x},t)|$. Thus, the origin of the whole system in (28) is globally asymptotical stable. In addition, the control law given in (30) makes output $y(t)$ of the system in (11) globally asymptotically track the reference trajectory. It means that $e\to 0$ and $s\to 0$ as $t\to\infty$.

4. EXPERIMENTAL APPLICATIONS AND RESULTS

In order to validate the effectiveness of the proposed backstepping sliding mode controller, it is implemented to the real electromechanical system described previously in section 2. For comparison purposes, the sliding mode controller and the backstepping controller designed in the foregoing section are also implemented to the real system. In the real system, the output angular velocity $\omega(t)$ is measured by a tachometer. Due to the lack of a sensor to measure the acceleration $\dot{\omega}(t)$, the other state variable, it is simply obtained by numerical derivative of the velocity instead of designing an observer for it. In order to escape high measurement noise, a low-pass filter with the transfer function of $G_f(s)=\frac{100}{s+100}$ is used. The saturation function in (25) rather than the signum function is utilized for the switching control $u_{sw}(t)$ due to its chattering reduction property. In view of consistency among the results, the controller parameters are selected to be equal $c_1=k_1=\varrho_1$ and $k_2=\varrho_2$ since they have similar characteristics if one takes a closer look at the control laws in (17), (22) together with (25), and (30). The parameters K_{bs} and ε_{bs} of the BSMC are chosen same as those of the SMC ($K_{bs}=K_s$ and $\varepsilon_{bs}=\varepsilon_s$), respectively. The controllers are tested for different matched uncertainty values of $\nabla=0$, $\nabla=-0.05$, and $\nabla=-0.1$ to show their behaviors against uncertainties. For all experiments, the values of the controller parameters $c_1=k_1=\varrho_1=600$, $k_2=\varrho_2=10$, $K_{bs}=K_s=3\times10^6$, and the initial conditions $\mathbf{x}(0)=[x_1,x_2]^T=[\omega,\dot{\omega}]^T=[0,0]^T$ of the electromechanical system are used. A step reference trajectory of 1250 rpm in magnitude is applied to the control systems for all experiments.

The responses of the controllers to a step reference of 1250 rpm are shown in Fig. 3a and 3b for the controller parameters

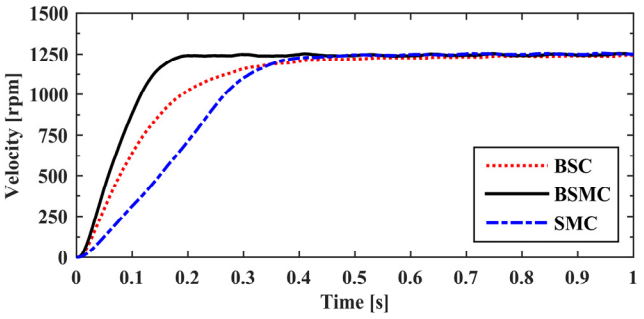

(a)

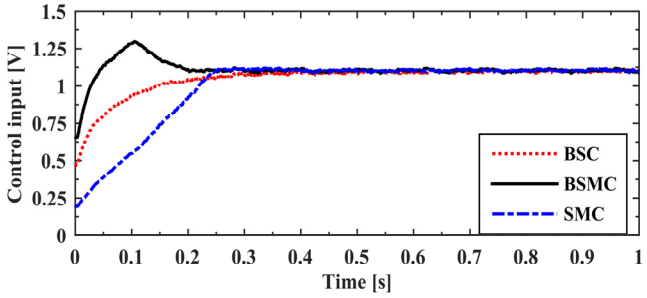

(b)

Fig. 3. Experimental results for nominal model with the matched uncertainty $\nabla=0$ and $\varepsilon_{bs}=\varepsilon_s=2\times10^5$: (a) Angular velocity, (b) Control input.

$\varepsilon_{bs} = \varepsilon_s = 2\times10^5$. In this experiment, the nominal model with the matched uncertainty $\nabla = 0$ for the electromechanical system is assumed. The performance of the BSMC according to rise time and settling time is much better than those of the BSC and SMC. The BSMC and SMC exhibit almost same steady-state error about 10 rpm while BSC does much larger about 17 rpm. As can be seen in Fig. 3a, the BSMC is the fastest in response. The settling time for the BSMC is approximately 0.2 s but those for BSC and SMC are about 0.4 s. Almost no overshoot is observed for three controllers. Input signals of the three controllers converge with different speeds as shown in Fig. 3b. The BSMC has a faster control signal than the others. Moreover, the BSMC input increases higher level than the others in transient regime, staying within its bound of $\left|2.5\right|$ V. This behavior contributes a faster response to the control system.

Let us now discuss behaviors of the controllers under the matched uncertainty $\nabla = -0.05$ for the electromechanical system. The aim of the experiments is to compare performances of the three controllers, the BSC, SMC, and BSMC for robustness against model parameter uncertainty. Experimental results for the control system with the matched uncertainty $\nabla = -0.05$ are depicted in Fig. 4 for the controller parameters $\varepsilon_{bs} = \varepsilon_s = 2\times10^5$. The shorter rise and

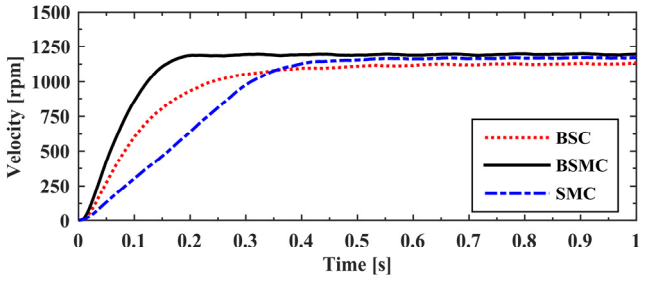

(a)

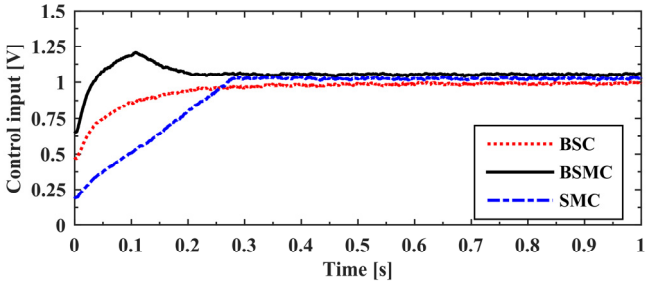

(b)

Fig. 4. Experimental results for uncertainty $\nabla = -0.05$ and $\varepsilon_{bs} = \varepsilon_s = 2\times10^5$: (a) Angular velocity, (b) Control input.

settling times and smaller steady-state error are obtained from the proposed BSMC as compared with the BSC and SMC as seen in Fig. 4(a). All controllers do not show overshoot. Settling times and steady-state errors are about 0.2 s and 60 rpm, respectively, for the proposed BSMC, 0.35 s and 110 rpm, respectively, for the BSC, and 0.4 s and 85 rpm, respectively, for the SMC. It is obvious that the BSMC has less output variation from trajectory in steady-state compared to the BSC and SMC. This ensures that under parametric uncertainties the BSMC is more robust than the BSC and SMC. It can be observed from Fig. 4(b) that the BSMC control law strives to track the reference trajectory more closely than those of the BSC and SMC when a parametric uncertainty exists. As can be seen from the figure, it is easy to understand that the unwanted high frequency chattering existing in the control input is considerably less in the cases of the BSMC and SMC, and almost same as in the case of the BSC because of chattering reduction attribute of the saturation function used in switching control laws of the BSMC and SMC. From the point of view of the chattering free control, the BSMC and SMC compete against the BSC when the saturation function is used.

The last experiment is done to be able to make a more precise remark on robustness of the proposed control system. In order to check robustness and transient speed of the control system, the parametric uncertainty constant ∇ is set to -0.1 for more uncertainties. Thus, nominal model uncertainty is increased by 10 percent. In this case, behaviors of the controllers become more pronounced as is shown in Fig. 5 for the controller parameters $\varepsilon_{bs} = \varepsilon_s = 2\times10^5$. The steady-state errors are approximately 100 rpm, 150 rpm, and 225 rpm for the BSMC, SMC, and BSC, respectively, as seen in Fig. 5(a). The settling times are about 0.2 s, 0.4 s, and 0.5 s for the BSMC, BSC, and SMC, respectively. The experimental results demonstrate no overshoot phenomenon

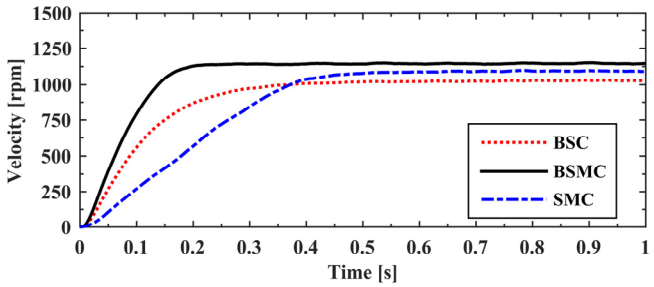

(a)

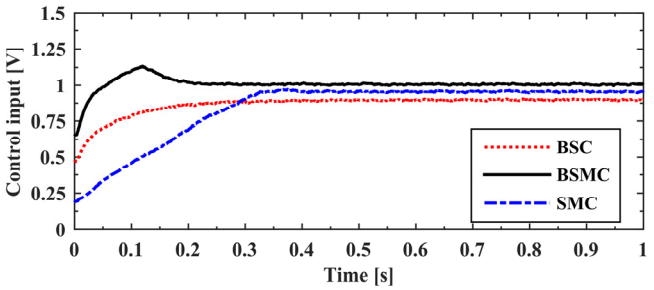

(b)

Fig. 5. Experimental results for uncertainty $\nabla = -0.1$ and $\varepsilon_{bs} = \varepsilon_s = 2\times10^5$: (a) Angular velocity, (b) Control input.

for the three controllers. From Fig. 5(b), it is not surprising that the control signals exhibit similar behaviors to those in the previously mentioned experiments. It is clear that the

control signals of the three controllers are almost smooth without chattering. Nevertheless, the BSMC control law provides faster and larger control signal than the other two controllers in transient and steady-state conditions.

As seen in Figs. 4 and 5, there exists almost no chattering, yet the control systems cannot track exactly the reference trajectory because of parametric uncertainty although they are stable. Nevertheless, precise tracking can be accomplished by adjusting the switching action of the BSMC and SMC. But it is not possible to do so for the BSC since it has no switching control part. Let us improve tracking error of the BSMC and SMC setting the controller parameters $\varepsilon_{bs} = \varepsilon_s = 2\times10^4$ for uncertainty $\nabla = -0.05$ and $\varepsilon_{bs} = \varepsilon_s = 2\times10^3$ for uncertainty $\nabla = -0.1$. The results are shown in Figs. 6 and 7. From the figures one can observe that the less tracking error for the control system with more uncertainty the more chattering. These tests demonstrate that robustness of the nonlinear plant under sliding mode control with respect to uncertainties and disturbances is improved at the cost of chattering in these practical situations. As seen Figs. 6(a) and 7(a) the BSMC and SMC closely track the reference trajectory but the BSC does not. From Figs. 6(b) and 7(b) one can see that the BSMC and SMC produce similar chattering effect to make the electromechanical system output track the reference trajectory. This indicates the robustness of the BSMC in the existence of uncertainty and disturbance. The BSMC is not only faster in response than the BSC and SMC but also more robust than the BSC. This is evidenced by the fact that it takes the robustness and disturbance rejection properties of

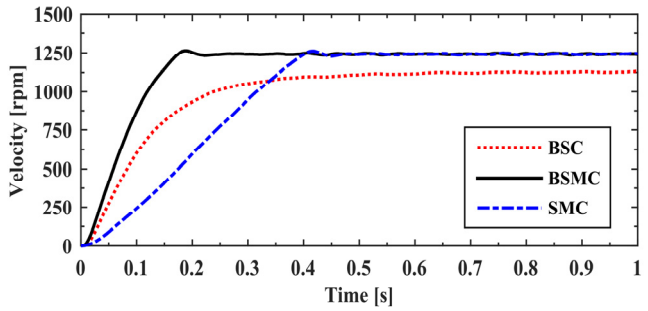

(a)

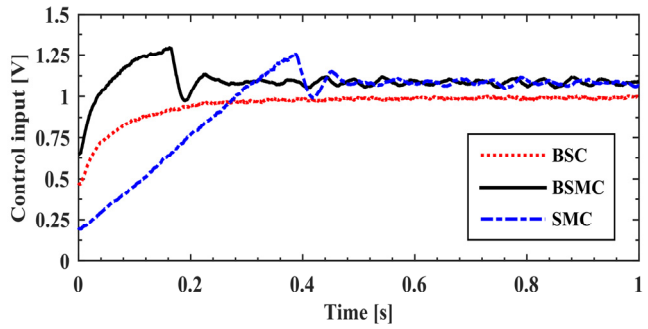

(b)

Fig. 6. Experimental results for uncertainty $\nabla = -0.05$ and $\varepsilon_{bs} = \varepsilon_s = 2\times10^4$: (a) Angular velocity, (b) Control input.

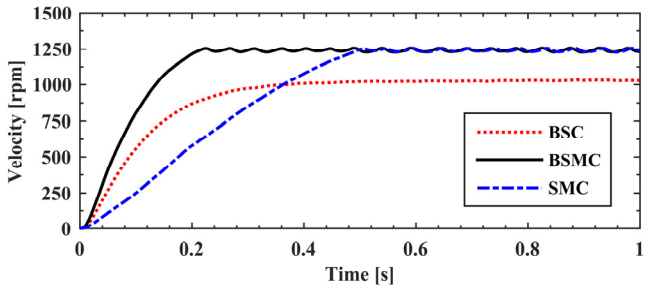

(a)

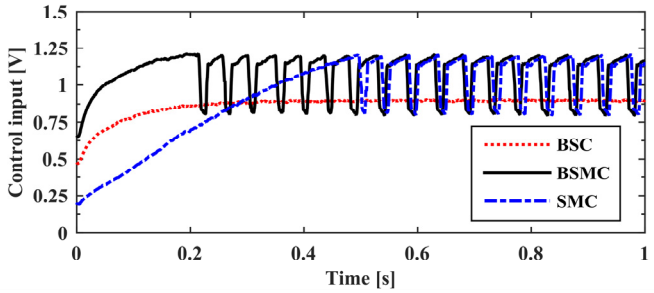

(b)

Fig. 7. Experimental results for uncertainty $\nabla = -0.1$ and $\varepsilon_{bs} = \varepsilon_s = 2\times10^3$: (a) Angular velocity, (b) Control input.

the SMC and fast response property of the BSC at the same time. It is clear that the main difference between the BSMC and the SMC is that the BSMC has tracking error term in its control law but the SMC does not. In other words, their equivalent control parts are different while their switching control parts are the same. It is easy to say that the BSMC differs from the BSC as to switching control part.

5. CONCLUSION

In this paper, backstepping sliding mode controller (BSMC) for an electromechanical system is proposed in order to resolve the difficulties in nonlinearity, uncertainty and external disturbance affecting it. Comparisons with different controllers which are conventional sliding mode controller (SMC) and backstepping controller (BSC) for angular velocity control are presented. Furthermore, stability of the control system is verified by Lyapunov direct (second) method.

In order to show effectiveness of the three controllers, they are implemented on the real electromechanical system. Some experiments are carried out to test robustness of the controllers for different uncertainty parameter values. According to the experimental results the proposed BSMC offers an improvement in steady-state error compared to the BSC and SMC. The BSMC gives satisfactory transient performance in terms of rise time and settling time, eliminates overshoot, and keeps steady-state error as minimum as possible. Both a faster transient response and a smaller steady state error for trajectory tracking are obtained by the BSMC. Furthermore, the BSMC rejects disturbance and improves robustness against parametric uncertainty.

The obtained experimental results demonstrate that the BSMC is simply implemented, and its performance and robustness are better than the conventional SMC and BSC. From the experimental results, it is concluded that the control performance and robustness of the electromechanical system is considerably enhanced with the BSMC.

REFERENCES

Adhikary, N. and Mahanta, C. (2013). Integral backstepping sliding mode control for under actuated systems: Swing-up and stabilization of the Cart–Pendulum System. *ISA Transactions,* 52 (6), 870-880.

Bisztyga, B. and Sieklucki, G. (2012). Sliding mode control of the dc drive with relative degree higher than one. *Przegląd elektrotechniczny*, 88 (11a), 38-42.

Chaouch, S. and Nait-Said, M.S. (2006). Backstepping control design for position and speed tracking of dc motors. *Asian Journal of Information Technology,* 5 (12), 1367-1372.

Damiano, A., Gatto, G.L., Morungiu, I, and Pisano, A. (2004). Second-order sliding mode control of DC drives. *IEEE Transactions on Industrial Electronics,* 51 (2), 354-373.

Davila, J. (2013). Exact tracking using backstepping control design and high-order sliding modes. *IEEE Transactions on Automatic Control,* 58 (8), 2077-2081.

Espinoza, T., Dzul, A.E., Lozano, R., and Parada, P. (2014). Backstepping-sliding mode controllers applied to a fixed-wing UAV. *Journal of Intelligent & Robotic Systems*, 73 (1), 67–79.

Guo, J., Ji, J., Yang, F., and Yao, B. (2012). Adaptive robust control for servo system with friction and input dead-zone nonlinearity. In: *Proceedings of International conference on modelling, identification and control,* 993-997.

Kesarkar, A.A. and Selvaganesan, N. (2013). Fractional control of precision modular servo setup for better limit cycle suppression. In: *Proceedings of IEEE International conference on control applications (CCA),* 467-471.

Khalil, H.K. (2015). *Nonlinear control*. Pearson Education Inc., Upper Saddle River, NJ.

Krstic, M. and Smyshlyaev, A. (2008). *Boundry control of PDEs: a course on backstepping designs*. Siam, Philadelphia.

Krstic, M., Kanellakopoulos, I., and Kokotovic, P. (1995). *Nonlinear and adaptive control design*. Wiley, New York.

Liu, J. and Wang, X. (2012). *Advanced sliding mode control for mechanical systems: Design, analysis and Matlab simulation*. Springer-Verlag, Berlin Heidelberg.

Lu, C-H., Hwang, Y-R., and Shen, Y-T. (2011). Backstepping sliding mode tracking control of a vane-type air motor table motion system. *ISA Transactions,* 50 (2), 278–286.

Madani, T. and Benallegue, A. (2006). Backstepping sliding mode control applied to a miniature quadrotor flying robot. In: *Proceedings of the IEEE 32'nd annual conference on Industrial Electronics (IECON 2006),* 700-705.

Payam, A.F. and Dehkordi, B.M. (2006). Nonlinear sliding-mode controller for sensorless speed control of dc servo motor using adaptive backstepping observer. In: *Proceedings of International conference on power electronics, drives and energy systems (PEDES '06)*, 1-5.

Precision modular servo control experiments manual, Feedback Instruments, UK.

Rajendran, S. and Jena, D. (2015). Backstepping sliding mode control of a variable speed wind turbine for power optimization. *Journal of Modern Power Systems and Clean Energy,* 3 (3), 402–410.

Rubagotti, M., Estrada, A., Castaños, F., Ferrara, A., and Fridman, L. (2011). Integral sliding mode control for nonlinear systems with matched and unmatched perturbations. *IEEE Transactions on Automatic Control,* 56 (11), 2699-2704.

Sahab, A.R. and Ziabari, M.T. (2012). Generalized backstepping control for dc motor. In: *Proceedings of International conference on systems, signal processing and electronics engineering (ICSSEE'2012)*, 188-193.

Slotine, J.J. and Li, W. (1991). *Applied nonlinear control*. Prentice Hall Inc., Englewood Cliffs, New Jersey.

Tao, G. and Kokotovic, P. (1994). Adaptive control of plants with an unknown deadzones. *IEEE Transactions on Automatic Control,* 39 (1), 59-68.

Utkin, V., Guldner, J., and Shi, J. (2009). *Sliding mode control in electro-mechanical systems*. CRC Press, Boca Raton.

Zhonghua, W., Lin, B.C., and Shusheng, Z. (2006). Robust adaptive dead zonecompensation of DC servo system. *IEE Proceedings-Control Theory and Applications*, 153 (6), 709–713.

Zinober, A. and Liu, P. (1996). Robust control of nonlinear uncertain systems via sliding mode with backstepping design. In: *UKACC international conference on control*, 281–286.